MOLECULAR AND CELLULAR BIOLOGY, Sept. 2011, p. 3593–3602 Vol. 31, No. 17
0270-7306/11/$12.00 doi:10.1128/MCB.00848-10

A Conditional Mouse Model for Measuring the Frequency of Homologous Recombination Events *In Vivo* in the Absence of Essential Genes▽‡

Adam D. Brown,[1,2]† Alison B. Claybon,[2]† and Alexander J. R. Bishop[1,2]*

Department of Cellular and Structural Biology, University of Texas Health Science Center at San Antonio, 7703 Floyd Curl Drive, San Antonio, Texas 78229,[1] and Greehey Children's Cancer Research Institute, University of Texas Health Science Center at San Antonio, 8403 Floyd Curl Drive, San Antonio, Texas 78229[2]

Received 22 July 2010/Returned for modification 6 September 2010/Accepted 15 June 2011

The ability to detect and repair DNA damage is crucial to the prevention of various diseases. Loss of function of genes involved in these processes is known to result in significant developmental defects and/or predisposition to cancer. One such DNA repair mechanism, homologous recombination, has the capacity to repair a wide variety of lesions. Knockout mouse models of genes thought to be involved in DNA repair processes are frequently lethal, making *in vivo* studies very difficult, if not impossible. Therefore, we set out to develop an *in vivo* conditional mouse model system to facilitate investigations into the involvement of essential genes in homologous recombination. To test our model, we measured the frequency of spontaneous homologous recombination using the pink-eyed unstable mouse model, in which we conditionally excised either *Blm* or full-length *Brca1* (breast cancer 1, early onset). These two genes are hypothesized to have opposing roles in homologous recombination. In summary, our *in vivo* data supports *in vitro* studies suggesting that BLM suppresses homologous recombination, while full-length BRCA1 promotes this process.

The necessity to replicate and repair the genome accurately has driven the evolution of a battery of DNA damage responses and repair mechanisms. For example, endogenous oxidative stress, a source of spontaneous DNA damage, has been estimated to result in approximately 10,000 oxidatively damaged DNA sites per cell per day (2). In addition to oxidative damage, errors in mammalian DNA replication are estimated to account for approximately 10 double-strand breaks (DSBs) per cell cycle (42). Furthermore, exogenous exposures can have an even greater effect on DNA integrity. If not repaired, DNA lesions can result in genomic instability, with the potential consequence of malignant transformation and/or apoptosis. The clearest example of this effect is observed in patients deficient in the ability to recognize, respond to, or repair DNA damage. Such persons have increased sensitivity to exogenous damages and an elevated incidence of cancer (18). It is now understood that homologous recombination (HR), one method of DNA repair encompassing both the high-fidelity homology-directed repair (HDR) and error-prone single-strand annealing (SSA), is often associated with DNA replication and is capable of repairing a wide variety of DNA lesions (9, 45). It is interesting to note that the typical rate of HR, 10^{-5} to 10^{-6} events per base pair per generation (46), is comparable to that of mutations per base pair per generation (10^{-4} to 10^{-6}) (63). Therefore, measuring the spontaneous occurrence of HR events *in vivo* in response to endogenous DNA damages in the context of various genomic integrity deficiencies provides a relevant and valuable tool for understanding disease etiology.

Several genes are suspected or known to be involved in maintaining genomic stability. Considering the fundamental requirement for maintaining genomic integrity, it is not surprising that many of the genes involved in DNA damage recognition, response, and repair are essential. *In vivo* examination of such genes in mouse is often restricted by their absolute requirement during development. The use of a Cre/*loxP* system allows the conditional deletion of genes of interest (including essential genes) in tissues of interest by expressing the Cre recombinase enzyme under a tissue-specific promoter, and this strategy has been used successfully in a wide variety of *in vivo* investigations (71). Here we have combined a Cre transgene, *Trp1-Cre*, which is specifically expressed during the development of the retinal pigment epithelium (RPE) of the eye (55), with the established pink-eyed unstable (p^{un}) mouse model. The RPE of the p^{un} mouse model can be used to assess the frequency of HR events *in vivo* (6, 8).

The basis of the p^{un} model is an internal, tandem duplication of 70 kb, encompassing exons 6 to 18 of the murine pigmentation gene known as *Oca2* or *p* (14, 60). This duplication renders the *p* gene nonfunctional in a recessive fashion and is phenotypically observed as a hypopigmented mouse with pink eyes (the cells of the RPE are transparent) and dilute coat color (13, 14). The spontaneous deletion of exactly one copy of the p^{un} duplication produces a revertant (or functional) *p* gene and can be observed as a pigmented spot on the RPE or fur. Such a perfect deletion event is most likely the product of an HR mechanism (14, 40), though it could potentially be the product of DNA polymerase template switching. Using a substrate similar to that used in the p^{un} assay (i.e., a duplication/

* Corresponding author. Mailing address: Department of Cellular and Structural Biology, University of Texas Health Science Center at San Antonio, 7703 Floyd Curl Drive, San Antonio, TX 78229. Phone: (210) 562-9000. Fax: (210) 562-9014. E-mail: BISHOPA@UTHSCSA.EDU.

† These authors contributed equally.

‡ Supplemental material for this article may be found at http://mcb.asm.org/.

▽ Published ahead of print on 27 June 2011.

deletion assay), studies with a yeast model suggest that different types of HR can be responsible for deletion-mediated repair. Such HR mechanisms include HDR events dependent upon RAD51 (e.g., intrachromatid exchanges) and SSA (37). Despite the fact that the initiating lesions leading to spontaneous p^{un} reversion are unknown and despite the limitations of the system with regard to tissue specificity and timing (during embryonic development), the p^{un} mouse model has proven to be a sensitive assay to measure somatic HR events, either spontaneously for different genetic backgrounds or following a wide variety of differently acting DNA damaging agents (9). Considering that the p^{un} assay is not restricted to clastogenic induction and that exogenous exposure induces events in locations that correlate with the cellular pattern of replication during development (7), it is reasonable to assume that p^{un} deletion events can be initiated in response to DNA replication fork arrest. Here we test our conditional p^{un} model by measuring the effect on spontaneous HR frequency following the conditional deletion of either *Blm* or full-length *Brca1* (breast cancer 1, early onset), two genes with opposing roles in HR (25, 58).

BRCA1 was the first identified hereditary breast cancer-associated gene (28, 53). Mutations in *BRCA1* are associated with a greatly increased incidence (as high as 87% for some mutations) of breast and ovarian cancers among women (16, 30, 35, 75). The mechanism of BRCA1 in tumor suppression appears to be through its involvement in maintaining genomic stability, particularly DNA double-strand break repair via HR. In fact, BRCA1 colocalizes and interacts with the HR protein RAD51 (64). More directly, it has been shown that mouse embryonic stem cells lacking full-length *Brca1* ($Brca1^{\Delta 11/\Delta 11}$) are defective at gene targeting and HR repair (both HDR and SSA) via the I-SceI assay (56, 57, 67).

$BRCA1^{\Delta 11}$ is a naturally occurring, highly conserved splice variant missing exon 11 (74). Exon 11 codes for about 60% of the BRCA1 protein, including key phosphorylation sites (27, 79), both of the nuclear localization sequences (68), and all or part of the protein-protein interaction domains for the HR proteins RAD51 (64), the MRE11/RAD50/NBS1 complex (81), and BRCA2 (80). Mice with a mammary-specific deletion of exon 11 (i.e., $\Delta 11/\Delta 11$ in mammary tissue only) develop mammary tumors that characteristically display genomic instability, such as chromosomal rearrangements (78).

Blm, the gene responsible for the rare autosomal disorder Bloom syndrome (BS) (32), is one of 5 human RecQ helicase family members (44). BS is an autosomal recessive disorder that clinically presents as growth retardation, immunodeficiency, facial and cranial abnormalities, reduced fertility, and increased cancer predisposition (39). The cancer phenotype observed in BS is unique in that it recapitulates the various malignancies observed in the general population (31, 38). The high incidence of cancer is believed to be caused by increased chromosomal instability, as exemplified by an approximate 10-fold increase in sister chromatid exchanges (SCEs) (19). An SCE indicates a DNA crossover event between two sister chromatids that is likely the result of HR (66). Due to the increase in SCEs in BS cells, BLM was initially hypothesized to be an antirecombinagenic protein, suppressing the frequency of spontaneous HR. More recently it has been proposed that BLM has both pro- and antirecombinogenic functions (25).

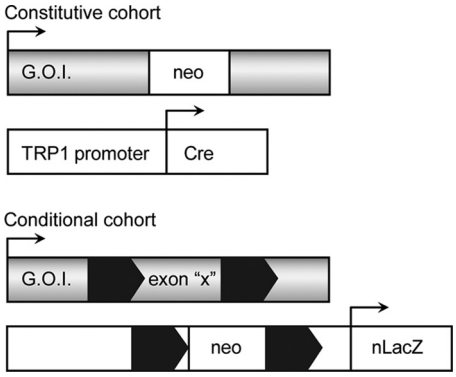

FIG. 1. Two-cohort breeding strategy used for each gene of interest (G.O.I.). Mice in the constitutive cohorts were heterozygous for a targeted null mutation (*neo* disrupted) of the G.O.I. and were homozygous for the *Trp1-Cre* transgene. Mice in the conditional cohorts were homozygous both for a targeted floxed (or conditional) allele of the G.O.I. (usually *loxP* sites flanking one or more exons of the G.O.I. [exon "x"]) and for the *RC*::*PFwe* β-galactosidase reporter. Noted are nuclear localized β-galactosidase (nLacZ), *loxP* sites (black pentagons), and transcription (arrows above the schematics).

Constitutive, homozygous deletion of either BLM or BRCA1 results in embryonic lethality, limiting *in vivo* experimentation (11, 24). In establishing our conditional p^{un} model, we first demonstrated that Cre recombinase has no effect on spontaneous HR frequency, as measured by p^{un} reversion events. Second, we found that conditional heterozygosity for either *Blm* or full-length *Brca1* does not result in an HR phenotype due to haploinsufficiency. Finally, we show that the loss of *Blm* results in a hyperrecombination phenotype, whereas the loss of full-length *Brca1* results in a hyporecombination phenotype. To our knowledge, this is the first *bona fide in vivo* mammalian study that shows BLM suppresses and BRCA1 promotes spontaneous HR frequency.

MATERIALS AND METHODS

Mouse lines and PCR genotyping. C57BL/6J and C57BL/6J $p^{un/un}$ mice were obtained from the Jackson Laboratory (Bar Harbor, ME). Mice carrying a targeted null allele of $Blm^{tm2Ches}$ (here referred to as Blm^{-}) (24) or a floxed allele of $Blm^{tm4Ches}$ (here referred to as Blm^{co}) (23) were obtained from P. Leder. When acted upon by Cre, the *Blm* floxed allele becomes effectively null. Mice carrying a targeted null allele of $Brca1^{tm1Cxd}$ (here referred to as $Brca1^{-}$) (65) or a floxed allele of $Brca1^{tm2Cxd}$ (here referred to as $Brca1^{co}$) (78) were obtained from the MMHCC mouse repository (Frederick, MD). When acted upon by Cre, the *Brca1* floxed allele produces the Δ*11* splice variant. *RC*::*PFwe* mice (34) carry a targeted reporter construct knocked into the *Gt(ROSA)26Sor* locus and were obtained from S. Dymecki. Lastly, mice carrying the transgenic *Trp1-Cre* expression construct (55) were obtained from P. Chambon.

All mouse lines were backcrossed five times to C57BL/6J mice, followed by two additional crosses to C57BL/6J $p^{un/un}$ mice. *Blm* and *p* do not segregate independently because they are 14 centimorgans apart on chromosome 7. Therefore, mice carrying either of the *Blm* alleles of interest required additional backcrosses to $p^{un/un}$. With these congenic C57BL/6J mice, the following breeding cohorts were established: (i) $Blm^{+/-}$ $Trp1\text{-}Cre^{tg/tg}$ $p^{un/un}$ (*Blm* constitutive), (ii) $Blm^{co/co}$ RC::$PFwe^{ki/ki}$ $p^{un/un}$ (*Blm* conditional), (iii) $Brca1^{+/-}$ $Trp1\text{-}Cre^{tg/tg}$ $p^{un/un}$ (*Brca1* constitutive), and (iv) $Brca1^{co/co}$ RC::$PFwe^{ki/ki}$ $p^{un/un}$ (*Brca1* conditional). Conditional heterozygous control (*co*/+) and experimental (*co*/−) offspring result from crossing the respective constitutive and conditional cohorts together. All offspring also carry *Trp1-Cre* and *RC*::*PFwe* and are homozygous for the p^{un} allele (Fig. 1). All animal studies were conducted in accordance with university and institute IACUC policies, as outlined in protocol 05054-34-01-A.

The $p^{un/un}$ genotype was identified by the phenotypic dilute coat color. All other genotypes were determined by PCR amplification using standard protocols

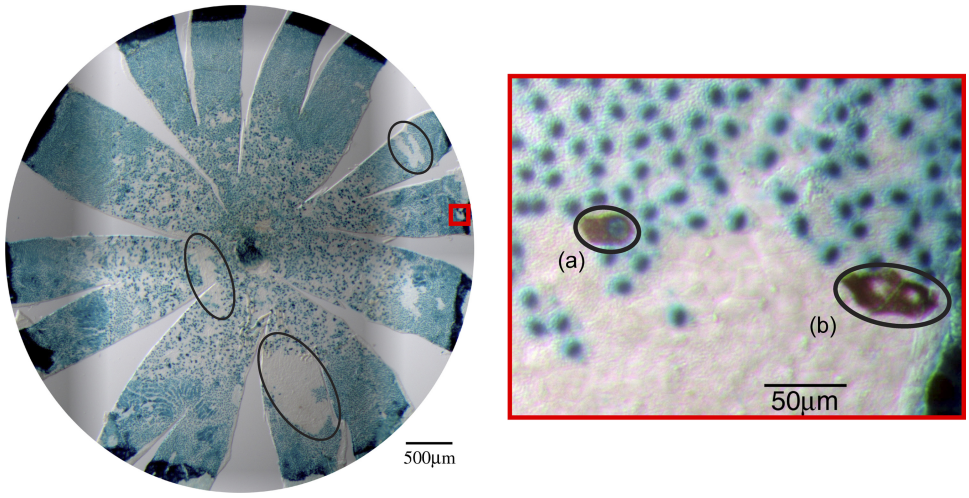

FIG. 2. *Trp1-Cre* control-stained RPE. The blue stain on the RPE indicates Cre activity in the nuclei of individual cells. The black ovals on the RPE outline areas of the RPE where Cre was not active, as indicated by lack of staining. The inset (outlined in red) depicts an HR event (brown melanin in cytoplasm) in which Cre has acted on the reporter allele (blue nucleus) (a) and an HR event (brown melanin in cytoplasm) in which Cre has not acted on the reporter allele (clear nuclei) (b).

as previously described (23, 24, 34, 55, 78), with the exception of *Trp1-Cre*. To distinguish *Trp1-Cre* hemizygosity from homozygosity, we performed quantitative PCR with the following primers: forward (5′-TTGCCGGTCAGAAAAA ATG) and reverse (5′-TCCAGGGCGCGAGTTG). One nanogram of DNA was used in the SYBR green PCR master mix reaction (Applied Biosystems, Foster City, CA), according to the manufacturer's instructions, and the cycling profile used was as follows: 1 cycle of 94°C for 5 min and 30 cycles of 94°C for 30 s, 60°C for 34 s, and 72°C for 34 s.

Dissection and staining of the retinal pigment epithelium. Harvesting and dissection of the RPE were carried out as previously described (7), with the following additions: after fixation, eyes were rinsed 3 times (for 10 min each) in phosphate-buffered saline (PBS) and stained for β-galactosidase activity in staining buffer (49) overnight at room temperature with gentle agitation. Destaining of eyes occurred through a series of 3 washes in PBS, with gentle agitation at room temperature for 30 min, 2 h, and overnight, respectively.

Visualizing and scoring reversion events on the retinal pigment epithelium. RPE whole mounts were visualized and imaged using a Zeiss Lumar version 12 stereomicroscope, Zeiss AxioVision MRm camera, and Zeiss AxioVision 4.6 software (Thornwood, NY). For each RPE, the percentage of nuclei with blue stain was used to assess β-galactosidase activity. The total number of eye spots and the number of cells making up that eye spot were recorded according to the criteria set forth by Bishop et al. (7).

Deletion PCR. To quantify Cre activity, we PCR amplified an excision product for the *Blm* and reporter alleles. The primers for the *Blm* allele were previously described (3). For the reporter allele we used the following primers: forward (5′-GGTTGAGGACAAACTCTTCGC) and reverse (5′-TCACCGGTGGGTG AAAAG). For both reactions, 50 nanograms of DNA isolated from paraformaldehyde-fixed RPEs using the DNeasy blood and tissue kit (Qiagen, Valencia, CA) was used, according to the manufacturer's instructions, and the cycling profile used was as follows: 1 cycle of 94°C for 5 min; 30 cycles of 94°C for 30 s, 60°C for 30 s, and 72°C for 1 min; and 1 cycle of 72°C for 3 min. Imaged PCR products were quantified using ImageJ software.

Statistical analysis. All statistics were carried using GraphPad Prism (La Jolla, CA). These include tests for normality (Shapiro-Wilk test), equal variances (F_{max} test), 2-group comparison (Mann-Whitney test, nonparametric *t* test), multiple group comparison (Kruskal-Wallis test, nonparametric one-way analysis of variance) with multiple comparisons *post hoc* (Dunn's test), contingency test (Fisher exact test), and tests of correlation (Spearman).

RESULTS

***Trp1-Cre* is active in the RPE but does not alter the frequency of p^{un} HR.** The p^{un} reversion model is a pigmentation-based assay. Following an HR event at the p^{un} mutation, brown melanosomes pack the cytoplasm, leaving a "clear" nucleus (Fig. 2). β-Galactosidase reporter constructs that are actively expressed only following Cre excision of a *loxP*-Stop-*loxP* cassette are often used to identify cells in which Cre has been active (12). Considering that the p^{un} reversion assay involves cytoplasmic location of melanin in RPEs, we utilized the *RC*::*PFwe* reporter mouse, which contains a Cre-activated nuclear localized β-galactosidase reporter (34). Thus, a cell with brown-pigmented cytoplasm and a blue nucleus is the result of a p^{un} HR event in which Cre has been active (Fig. 2). Using a group of control mice that carry both the *Trp1-Cre* transgene and the β-galactosidase reporter construct (*Trp1-Cre*$^{tg/o}$ *RC*::*PFwe*$^{ki/wt}$ $p^{un/un}$), we determined the relative proportion of blue staining on each RPE (data not shown). Our results demonstrate that *Trp1-Cre* activity is present, though the extent of activity varies for each RPE. Of note, we never observe RPEs with 100% of nuclei stained blue (Fig. 2). This finding points to the importance of using a Cre activity reporter in our conditional p^{un} reversion assay.

The RPE consists of a monolayer of approximately 55,000 cells (10). Earlier studies using the p^{un} assay report an average of ~5 to 6 eye spots per wild-type RPE (8, 10). In more recent studies, our laboratory reported a similar frequency of eye spot events in wild-type samples (17, 26). Considering that *Trp1-Cre* is expressed in the RPE and acts to recombine the genome at *loxP* sites, we questioned whether its expression affects spontaneous p^{un} reversion frequency. Using the *Trp1-Cre* control mice (*Trp1-Cre*$^{tg/o}$ *RC*::*PFwe*$^{ki/wt}$ $p^{un/un}$), we verified that the frequency of eye spots was not significantly different from that of wild-type $p^{un/un}$ controls using the traditional p^{un} frequency assay (Table 1; see also Fig. S1 in the supplemental material). Furthermore, the lack of difference we observed was regardless of our criteria for identifying eye spots (e.g., all eye spots, eye spots with blue nuclei, and eye spots with blue nuclei from RPEs exhibiting ≥80% blue staining [i.e., RPEs which display a high level of Cre activity]). Additionally, we found no significant correlation between the percentage of blue staining and

TABLE 1. Summary of RPEs examined and p^{un} reversion frequency by genotype

Genotype (criterion for eye spot identification)[a]	No. of RPEs	Total no. of eye spots	Avg no. of eye spots per RPE
Wild-type $p^{un/un}$	40	245	6.1
Trp1-Cre control (all)	32	165	5.2
Trp1-Cre control (only blue)	31	149	4.8
Trp1-Cre control (blue, ≥80% stain)	29	140	4.8
CC control (all)	74	387	5.2
CC control (only blue)	72	345	4.8
CC control (blue, ≥80% stain)	62	307	5.0
$Blm^{co/+}$ (all)	14	90	6.4
$Blm^{co/+}$ (only blue)	14	72	5.1
$Blm^{co/+}$ (blue, ≥80% stain)	9	51	5.7
$Blm^{co/-}$ (all)	36	621	17.3
$Blm^{co/-}$ (only blue)	35	546	15.6
$Blm^{co/-}$ (blue, ≥80% stain)	21	380	18.1
$Brca1^{co/+}$ (all)	28	132	4.7
$Brca1^{co/+}$ (only blue)	27	124	4.6
$Brca1^{co/+}$ (blue, ≥80% stain)	24	116	4.8
$Brca1^{co/-}$ (all)	30	82	2.7
$Brca1^{co/-}$ (only blue)	29	57	2.0
$Brca1^{co/-}$ (blue, ≥80% stain)	20	33	1.7

[a] All, all eye spots; only blue, eye spots with blue nuclei (Cre activity); blue, ≥80% stain, eye spots with blue nuclei from RPEs with ≥80% blue staining (Cre activity). The combined conditional (CC) control is the combination of the *Trp1-Cre* control with *Blm* and *Brca1* conditional heterozygote samples.

the number of eye spots per RPE (see Fig. S2 in the supplemental material). We therefore conclude that *Trp1-Cre* expression is active in the RPE and that its activity has no effect on the spontaneous frequency of HR events in the RPE, as measured by the p^{un} reversion assay.

Neither *Blm* nor *Brca1* conditional heterozygosity results in an altered HR frequency phenotype. Our experimental design involved crossing two groups of animals, a constitutive cohort and a conditional cohort, for each gene of interest (Fig. 1). The resulting offspring were either conditionally heterozygous ($Blm^{co/+}$ or $Brca1^{co/+}$; heterozygous control group) or conditionally null ($Blm^{co/-}$ or $Brca1^{co/-}$; experimental group). However, this design assumes that the conditional heterozygous genotype is equivalent to that of the wild type. We therefore examined whether the conditionally heterozygous loss of either *Blm* or full-length *Brca1* alters p^{un} reversion frequency. No significant difference in p^{un} reversion frequency was detected between either of the conditional heterozygous control groups compared to our *Trp1-Cre* control group (Fig. 3; Table 1). This result suggests that neither *Blm* nor *Brca1* conditional heterozygosity leads to an HR haploinsufficiency phenotype.

Conditional loss of *Blm* or full-length *Brca1* leads to an altered frequency of HR *in vivo*. After demonstrating that the conditional heterozygous groups have frequencies of p^{un} reversion equivalent to that of the wild type, we went on to examine the consequence of conditional loss of *Blm* or conditional loss of full-length *Brca1*. We directly compared the total frequencies of eye spots between the control genotypes and the conditional experimental genotypes. The conditional loss of *Blm* resulted in a significant increase in p^{un} reversion events ($P < 0.0001$; Kruskal-Wallis test). In contrast, conditional loss of full-length *Brca1* resulted in a significant decrease in p^{un} reversion events ($P < 0.0001$; Kruskal-Wallis test) (Table 1; see also Fig. S4A and B in the supplemental material). This clearly demonstrates that the conditional p^{un} assay system is able to observe both increases and decreases in HR frequency.

However, we wanted to explore how well the Cre reporter activity correlated with these gross changes in p^{un} reversion frequency. By examining the percentage of RPEs with β-galactosidase activity to p^{un} reversion frequency, we detected a significant positive correlation between increased blue stain and an increased number of eye spots per RPE in $Blm^{co/-}$ samples (Spearman $r = 0.6667$; $P < 0.0001$) (Fig. 4A). Considering the known requirement for BRCA1 in HR, it is not surprising that we also observed the result with the $Brca1^{co/-}$ RPE that was opposite of that seen with the $Blm^{co/-}$ RPE, a significant positive correlation between increased blue stain and a decreased number of eye spots per RPE (Spearman $r = -0.388$, $P = 0.0375$) (Fig. 4B). Despite this strong phenotypic correlation between the β-galactosidase Cre reporter activity and the expected HR phenotype, we wanted to further validate these results with a molecular analysis. We therefore examined the level of Cre excision of both the reporter construct and the *Blm* floxed allele by PCR amplification using DNA isolated from a fixed RPE monolayer isolated from a $Blm^{co/-}$ RPE that displayed differing amounts of blue stain (see Fig. S3A in the supplemental material). Quantification of these products showed that excisions of both floxed alleles by Cre are equivalent (Fig. S3B). Taken together, these results indicate that the β-galactosidase Cre reporter construct is indeed a good indicator of Cre activity on the gene of interest. Therefore, by only considering eye spots with blue nuclei (in which Cre has acted on the gene of interest), a more accurate assessment of HR in these models can be achieved. Doing so results in an outcome similar to the one seen previously: a significant increase in HR in the *Blm* experimental group ($P < 0.0001$; Kruskal-Wallis test) and a significant decrease in HR in the *Brca1* experimental group ($P < 0.0001$; Kruskal-Wallis test) (Table 1; see Fig. S4A and B in the supplemental material).

In pursuing the above logic, it would seem reasonable to use the β-galactosidase reporter activity to indicate those RPEs which best represent the conditional genotype of interest. Similar to the conditional controls, neither of the experimental groups displayed 100% staining. However, the variation in

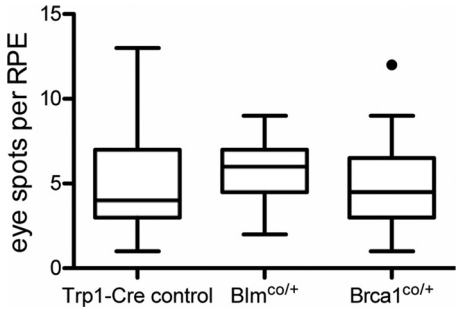

FIG. 3. Haploinsufficiency of either *Blm* or full-length *Brca1* does not alter HR frequency. Eye spots with blue nuclei from RPEs exhibiting ≥80% blue staining (Cre activity) were analyzed for HR frequency. No significant difference ($P = 0.371$; Kruskal-Wallis test) was detected when either *Blm* or *Brca1* conditional heterozygotes were compared to controls. Data are represented as Tukey box and whisker plots.

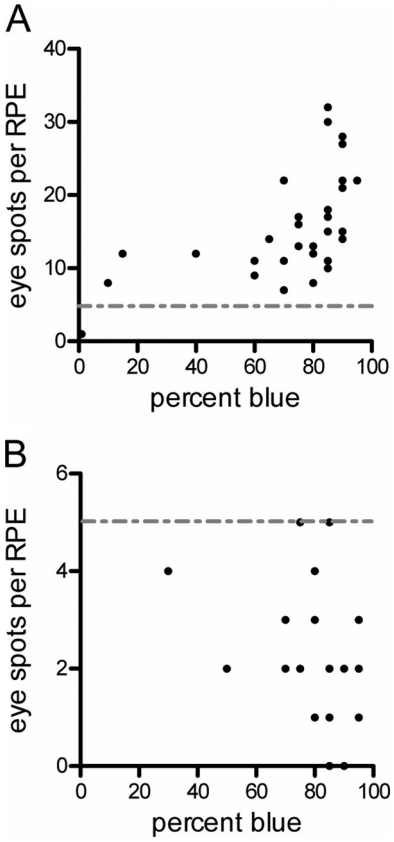

FIG. 4. Conditional loss of null alleles correlates with changes in HR frequency. (A) The conditional loss of *Blm*, as measured by the percentage of blue-stained RPEs (Cre activity), positively correlates with an increase in HR frequency (eye spots) (Spearman $r = 0.6667$; $P < 0.0001$). (B) The conditional loss of full-length *Brca1*, as measured by the percentage of blue-stained RPEs (Cre activity), positively correlates with a decrease in HR frequency (eye spots) (Spearman $r = -0.388$; $P = 0.0375$). (A, B) The dotted gray line emphasizes the average frequency of HR events per RPE (~5).

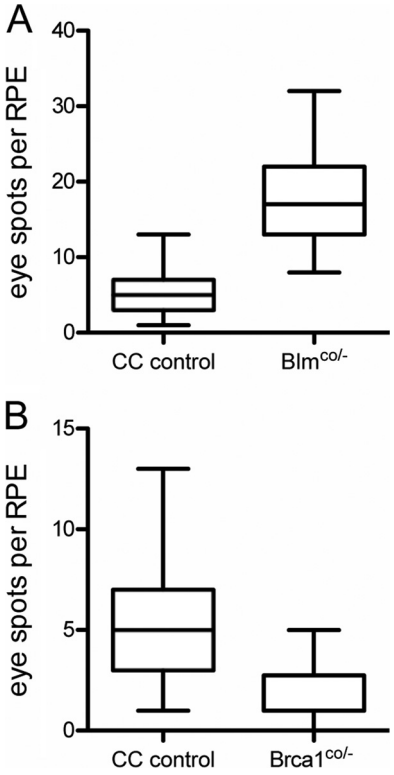

FIG. 5. Loss of *Blm* or full-length *Brca1* results in an increase or decrease in HR frequency, respectively. (A, B) Eye spots with blue nuclei from RPEs exhibiting ≥80% blue staining (Cre activity) were analyzed for HR frequency. Conditional loss of *Blm* results in a significant increase ($P < 0.0001$; Mann-Whitney test) of HR (A), and conditional loss of full-length *Brca1* results in a significant decrease ($P < 0.0001$; Mann-Whitney test) of HR compared to that of the combined conditional (CC) control (B) (see the text for details). Data are represented as Tukey box and whisker plots.

staining was significantly different from the control group but not each other (data not shown). To mitigate this difference, we reanalyzed our data, using only those RPEs with ≥80% staining. This analysis confirmed our previous results regarding eye spot frequency, revealing an increase in HR in the *Blm* experimental group ($P < 0.0001$; Mann-Whitney test) and a decrease in HR in the *Brca1* experimental group ($P < 0.0001$, Mann-Whitney test) (Fig. 5A and B; Table 1). In summary, our results demonstrate that BLM suppresses and BRCA1 promotes spontaneous HR *in vivo*.

Conditional loss of *Blm* and full-length *Brca1* affects replication-tied HR *in vivo*. The p^{un} eye spot assay provides a direct indication of the HR frequency that occurred in the developing mouse RPE. However, additional insights can be gained by examining the timing and pattern of these events observed within the RPE. For example, it is possible to distinguish between single- and multicell eye spots (Fig. 2) as well as when these events took place during development (see below). In a *Parp1* null background, we recently observed a significant increase in p^{un} reversion events, particularly multicell events (26). In the *Parp1* study, we suggested that the increase in multicell eye spots represents single-stranded DNA breaks that were repaired by HR in a DNA replication-dependent manner, which supports current models.

Similar to the *Parp1* null background, the hyperrecombination observed in $Blm^{co/-}$ RPEs is due to the significant increase in the number of multicell events compared to that in the control ($P = 0.0043$; Fisher exact test) (Fig. 6A). Conversely, the hyporecombination in $Brca1^{co/-}$ RPEs is due to the significant decrease in the number of multicell events compared to that in the control ($P = 0.0076$; Fisher exact test) (Fig. 6B) These results suggest that BLM acts to suppress the frequency of spontaneous HR events that are associated with DNA replication, while full-length BRCA1 is necessary for these same events. Interestingly, our results also indicate that there is a subset of proliferation-independent p^{un} reversion events that are not dependent upon the presence of full-length *Brca1*.

Blm suppresses spontaneous HR during early mouse embryonic development. The RPE begins to form in the developing eye cup around embryonic day 8.5 (E8.5) and continues on through the first week of postnatal life (33, 59). This development has been described as "radially outward from the optic nerve with an edge-biased pattern that has a churning motion" (10). Therefore, we can retrospectively define when these reversion events occur, similar to using the concentric circles for

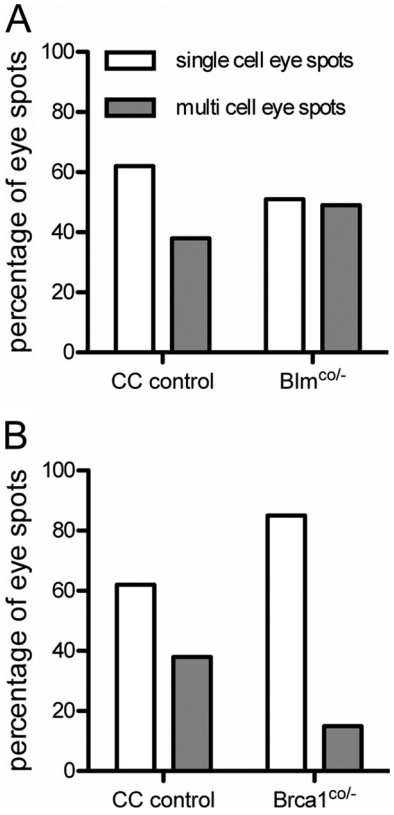

FIG. 6. Loss of *Blm* or full-length *Brca1* effects replication-tied HR events. (A and B) Eye spots with blue nuclei from RPEs exhibiting ≥80% blue staining (Cre activity) were analyzed for the occurrence of single-cell versus multicell HR events. Loss of *Blm* leads to a significant increase ($P = 0.0043$; Fisher exact test) in the percentage of multicell HR events compared to that of the CC (combined conditional) control (A), and the absence of full-length *Brca1* leads to a significant decrease ($P = 0.0076$; Fisher exact test) (B). Data are represented as the percentages of single-cell HR events (open bars) and multicell HR events (gray bars) for each genotype.

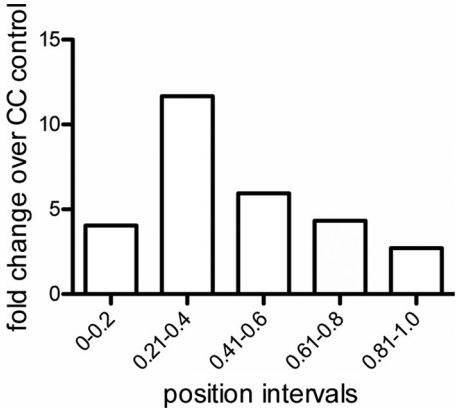

FIG. 7. Loss of *Blm* increases HR frequency early during mouse embryonic development. Multicell events from RPEs with ≥80% blue staining (Cre activity) were analyzed for the positional effect of HR frequency. A position of 0 is equivalent to the optic nerve, compared to a position of 1.0, which is equivalent to the outer edge of the RPE. A significant increase of multicell HR events ($P = 0.015$; Fisher exact test) was detected in the region of the developing RPE, corresponding to the interval 0.21 to 0.40 of *Blm* null mice compared to the CC (combined conditional) control. Data are represented as fold changes of *Blm* null HR over CC control HR.

aging trees (7, 17, 26). As such, p^{un} reversion events that occur close to the optic nerve must have arisen earlier in development than more distal events, which must have occurred later. In order to test whether or not the increase of multicell reversion events observed in the absence of BLM was restricted to a specific time during development, we first compared the relative positions of these multicell events between control and $Blm^{co/-}$ samples and found the distributions to be significantly different (data not shown). Examination of the distribution of locations of the multicell HR events revealed a significant increase in the $Blm^{co/-}$ samples compared to that in the control for the regions encompassing 0.21 to 0.4 ($P = 0.015$; Fisher exact test) (Fig. 7). This result suggests that BLM has its greatest effect on suppression of HR during early development, very reminiscent of our observations with PARP1.

DISCUSSION

The appropriate recognition and repair of DNA damage is imperative for maintaining genomic stability. In fact, many DNA damage response or repair genes are essential or their mutation results in inherited diseases that often lead to malignant transformation (18). Therefore, understanding the role of such genes *in vivo* constitutes the basic knowledge of crucial cellular processes and is key to identifying novel means to treat a variety of diseases, including cancer. HR is one such process that has the capacity to accurately repair a variety of DNA lesions that arise from endogenous and exogenous insults (9, 45). Thus, we set out to develop an *in vivo* conditional system to investigate the involvement of essential genes in HR.

Due to the embryonic lethality observed as a result of the constitutive knockout of BLM (24) or BRCA1 (11) in mouse, elucidating the *in vivo* function of these genes during normal somatic proliferation has proven difficult. Studies prior to ours have utilized *in vitro* and biochemical approaches, as well as model organisms other than the mouse, to understand the role of BLM and BRCA1 in HR. Plasmid-based recombination assays have shown that BRCA1 promotes HR (56, 57, 67) and that BLM suppresses HR (73). BRCA1 and BLM have also been shown to interact with RAD51 following DNA damage as well as during DNA replication (5, 20, 47, 64, 76) (discussed below). Using synthetic DNA structures, BLM was found to preferentially act on DNA structures (e.g., 4-way synthetic Holliday junctions) (45), which gave way to the finding that BLM has a major role in preventing crossovers by dissolution of a double Holliday junction (DHJ) structure (54) (Fig. 8F). In addition to the helicase activity, BLM also has a strand annealing capability (22, 50). The latter activity of BLM can facilitate regression of a stalled replication fork or template switching by annealing the nascent strands (leading and lagging) at the replication fork, thereby giving rise to the "chicken foot" structure (Fig. 8A) (61). It has also been shown that BLM helicase activity can promote Holliday junction branch migration, and if this is in the direction of the stalled fork, it will restore the replication fork (Fig. 8C and D) (48, 51, 61). Furthermore, the *Drosophila* ortholog of BLM (DmBlm) was found to suppress crossovers by also promoting synthesis-de-

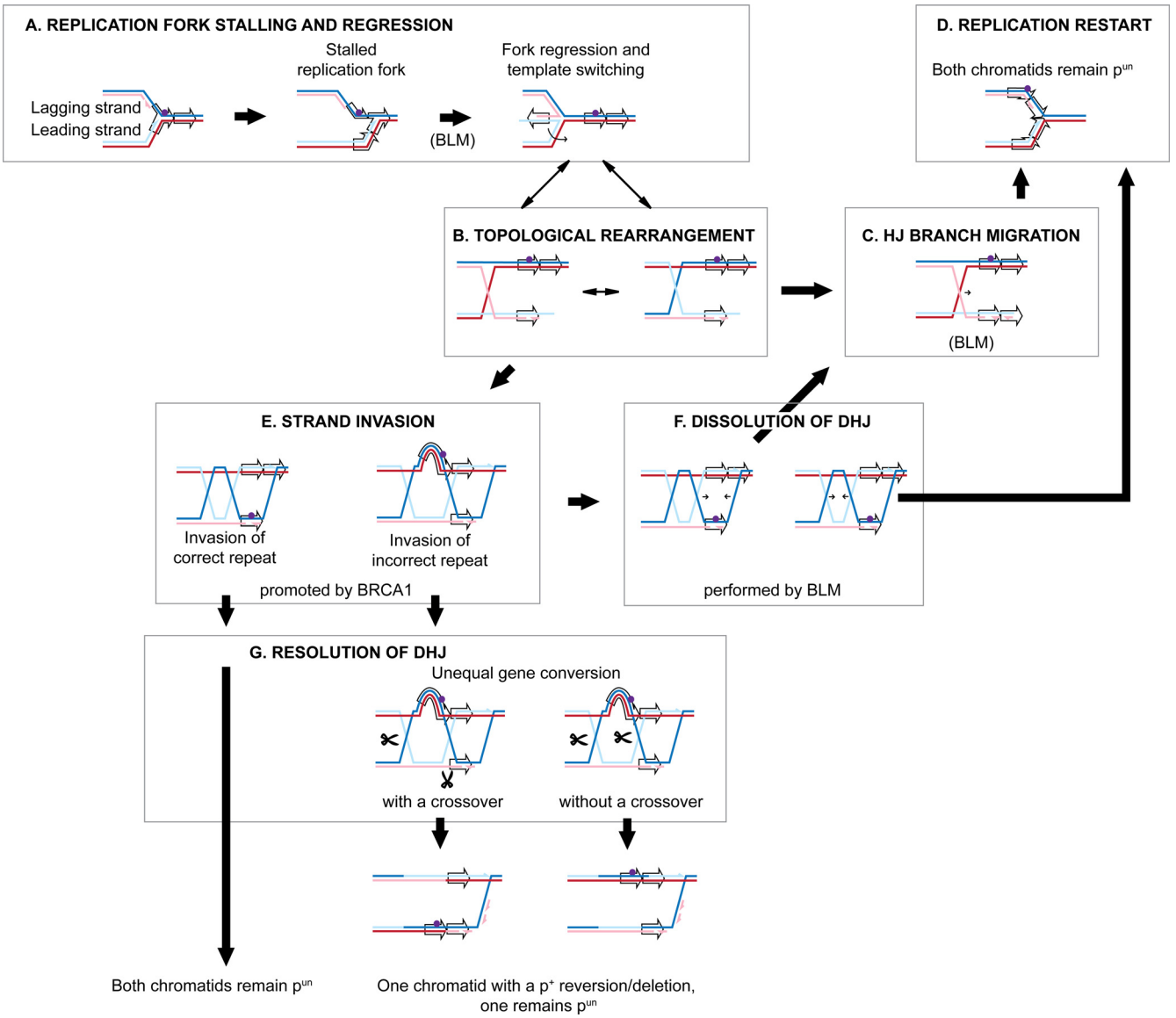

FIG. 8. Model for DNA replication restart in the context of a repeated DNA segment such as p^{un} in either a BLM-dependent or -independent manner. Presented is the occurrence of DNA damage that blocks lagging-strand DNA replication at the first repeat of DNA duplication, though similar models can be drawn for damage in the second repeated DNA element or that affect leading-strand synthesis. Complementary parental DNA strands (dark red and blue) and their nascently replicated leading and lagging strands (light blue and light red, respectively) are shown. DNA replication is indicated by a half arrowhead, DNA damage as a purple circle, and the repeated DNA elements by outlined black arrows. (A) Following damage-induced stalling of the replication fork, regression can occur (or template switching) by annealing the nascent strands to form a "chicken foot" structure possibly mediated by BLM (in parentheses, as other proteins such as Werner helicase can promote this activity). Using the nascent leading strand as a template, the lagging strand can now be extended beyond the DNA lesion found on the blue parental DNA strand. (B) Topological rearrangement. The "chicken foot" structure is topologically the same as a Holliday junction (HJ). (C, D) HJ branch migration (C), which can be mediated by BLM helicase, among others, can reverse the regressed fork, allowing replication restart (D). Of note, this mechanism would inhibit repeat duplication deletion, would not involve sister chromatid exchange, and would be limited by the amount of leading strand template available to bypass the lesion present on the parental strand. (E) Alternatively, the annealed nascent strands at the regressed replication fork would have a 3′-end overhanging tail that can be used for RAD51-dependent strand invasion promoted by BRCA1, resulting in strand displacement (a "D-loop") and, consequently, the production of two additional HJs once the D-loop is captured by the nascent lagging strand. If the 3′-end tail is complementary to the repeated DNA element, then there is the chance that it can invade into the "correct repeat" or the "incorrect repeat." (F) Irrespective of which repeat is invaded, BLM can dissolve a double HJ (DHJ) by migrating two HJs toward each other. Depending on which DHJ is dissolved, either a regressed replication fork is reformed that can be resolved by HJ branch migration or the replication fork is restored, without any possibility of either chromatid exchanges or repeat deletions in either case. (G) An alterative means to dissolve a DHJ is by resolution. The orientation of HJ resolution (cutting red HJ/red HJ or blue HJ/blue HJ versus cutting red HJ/blue HJ) will dictate whether or not resolution results in strand exchange. Irrespective of the resolution orientation, invasion of the 3′-end tail into the "correct" or "incorrect" repeat will dictate the possibility of repeat deletion (e.g., p^{un} reversion, in the case of our assay).

pendent strand annealing, another subtype of HDR that occurs following DSBs (1, 43, 52).

Here we were able to take advantage of conditional knockout mouse models of *Blm* and full-length *Brca1* to determine the consequence of removing either gene on HR using the established p^{un} mouse model. Mice lacking *Blm* displayed an increased frequency of HR (Fig. 5A), while mice lacking full-length *Brca1* displayed a decreased frequency of HR (Fig. 5B).

Our conditional p^{un} assay capitalizes on the tissue-specific activity of Cre recombinase to cleave and recombine DNA at a specific sequence. Bioinformatic analysis of the mouse genome has revealed that pseudo-*loxP* sites exist in the mouse genome and support Cre activity (69). First we validated that Cre activity did not effect RPE development or spontaneous HR frequency. An interesting observation is that irrespective of genotype, we never obtained any RPE that appeared to have 100% blue staining (denoting Cre activity). This is of particular importance regarding the conditional loss of our genes of interest. Mouse ocular development has been detected as early as E8.0 (36), and *Trp1*, the promoter driving Cre expression in our system, is known to be expressed as early as E11.0 of mouse development (62). Therefore, it is plausible that some selective advantage for clear cells (i.e., cells that did not express Cre and presumably also retain one functional copy of either *Blm* or *Brca1*) could occur in the developing RPE. However, some degree of cellular proliferation can occur even following the complete loss of either BLM or full-length BRCA1, as evident by this study and more importantly by the fact that BLM null and BRCA1 homozygous mutant embryos survive until developmental E13.5 and E12.5, respectively (24, 77). Additionally, one could speculate that a pigmented RPE spot with blue nuclei could result from an HR event that occurred before Cre activity took place (i.e., before the gene of interest was deleted). Experimentally, this would be difficult to refute. We empirically showed that the change in frequency of HR correlates well with the amount of stain present (i.e., the loss of either *Blm* or full-length *Brca1*) (Fig. 4A and B). To further confirm that our reporter is an accurate indicator for excision of both the reporter and the floxed allele of the gene of interest, we used a PCR-based approach to amplify each of the alleles following Cre excision activity and found that Cre acts equally at both sites (see Fig. S3 in the supplemental material).

Epidemiological studies involving carriers of either mutated BLM or BRCA1 suggest that heterozygous loss of one copy of either gene leads to an increased propensity to develop cancer (15, 53). This observation suggests the possibility that heterozygous loss of either *Blm* or *Brca1* could impact the frequency of HR. We therefore tested for an HR haploinsufficiency phenotype but found no difference in the HR frequency for conditional heterozygous loss of either gene (Fig. 3). Our *in vivo* findings complement those of Chester et al., which showed levels of SCEs from *Blm* heterozygous mouse embryonic fibroblasts that were not different from wild-type controls (24).

Although the loss of full-length *Brca1* leads to a significant decrease in the frequency of HR (Fig. 5B), we did detect a number of reversion events following Cre activity. We classify a reversion event as either being comprised of a single cell (1 cell) or a clonally expanded cluster of cells ($\geq$2 cells) (7). Therefore, we can also ask if the loss of full-length *Brca1* affects single-cell and/or multicell HR events. Of the HR events detected in the *Brca1* experimental group, the majority were single-cell events (Fig. 6B). For comparison, Claybon et al. found that the increase of HR events in the absence of PARP1 was due primarily to large multicell events (26). *Brca1* expression is induced prior to DNA synthesis and stays abundant during S and G_2 phase (21, 41, 70). In addition to Brca1 expression during replication, BRCA1 forms discrete nuclear foci with RAD51 during S phase and with PCNA in response to DNA damage that can stall a replication fork (21, 47, 64). In fact, BRCA1 directly interacts with RAD51 (64). Further, it should be noted that PARP1 inhibition is synthetic lethal with BRCA1 deficiency (29), most likely due to the lack of PARP1-dependent single-strand break repair, leading to increased stalled replication forks that cannot be repaired in a BRCA1 HR repair-dependent manner. Considering these previous observations and the results from this study in combination with the study by Claybon et al., we hypothesize that p^{un} revertant multicell events are the outcome of HR events tied to replication and that at least a majority of the single-cell events are not (26). Furthermore, these replication-associated HR events are likely to be RAD51 dependent, whereas replication-independent HR resulting in p^{un} reversion is likely the result of a RAD51/BRCA1-independent SSA event. These *in vitro* studies support our *in vivo* observations that BRCA1-associated HR occurs in response to DNA damage, which results in replication stress.

It is interesting to note that the increase of HR following the loss of Blm that we report here occurred early during embryonic development (Fig. 7). Bishop et al. previously established that the location of a p^{un} reversion event in an adult RPE indicates the developmental time at which it arose by mapping the location of damage-induced p^{un} eye spots following *in utero* exposure at specific developmental timings (6). The greatest increase in p^{un} reversion events that we observed in the absence of BLM was in RPE region 0.21 to 0.4, which corresponds to a time before E13.5 during development. Chester et al. cited anemia as the potential cause of death in *Blm* null embryos beginning around E10.5 (24), and considering that the fetal liver is a highly proliferative hemopoietic tissue at that time, our observation suggests the possibility of catastrophic genomic instability due to an inability to efficiently repair stalled replication forks in the absence of BLM in this tissue at that time. The increase of genomic instability that we observed in the RPEs of BLM null mice is representative of other developing somatic tissues, and in fact, Chester et al. observed a significant increase in micronuclei in the fetal liver of developing *Blm* null embryos, suggesting the notion of increased genomic instability (24).

During the preparation of the manuscript, Wang et al. showed that the depletion of BLM in human fibroblasts led to an overall increase of HR and that the increase was most likely the result of an HDR crossover event rather than SSA (73). Our study also shows an overall increased frequency of HR in the absence of BLM (Fig. 5A) and that this increase manifested as multicell p^{un} reversion events (Fig. 6A), interpreted by us as resulting from replication-associated RAD51-dependent events. Therefore, both this study and that by Wang et al. suggest that BLM suppresses HDR rather than SSA events. We presume that these HDR events would be suppressed by

either reversal of a regressed replication fork (essentially a Holliday junction branch migration) or DHJ dissolution followed by reversal of a regressed replication fork. For our assay, it should be noted that reversal of a regressed stalled replication fork should not allow deletion of a p^{un} repeat. However, if that regressed stalled replication fork was repaired via resolution of a DHJ (Fig. 8E and G) following RAD51-mediated invasion into the "wrong" repeat (i.e., an unequal SCE event), this would produce a p^{un} deletion/reversion. Resolution of a DHJ would be the only mechanism available for the repair of a DHJ structure in the absence of BLM.

Studies using PARP1 inhibition have proven effective in patients that are defective in BRCA1 (29). This synthetic lethal approach is premised on the hypothesis that the inability to repair damaged DNA by HR (e.g., in many *BRCA1/2* mutant cancers) forces the cell to rely upon alternative mechanisms and, in the absence of such alternatives (e.g., resulting from PARP1 inhibition), will lead to cellular death. Recently, as shown in a paper by Claybon et al., our laboratory used the p^{un} HR model to show that the loss of PARP1 leads to a hyper-recombinagenic phenotype (26). This result, in combination with the present study, gives *in vivo* proof of concept for how PARP1 inhibition is an effective therapeutic against tumors displaying *BRCA*ness (4). If BLM resembles PARP1 with respect to HR, then perhaps the transient inhibition of BLM could also be considered a therapeutic strategy to BRCA1/2 breast and ovarian cancers. It is notable that BLM and BRCA1 have been found to interact with each other within the BRCA1-associated genome surveillance complex (72). Though the role of this interaction is not understood, it is interesting to speculate that their interaction may coordinate the determination for whether HDR is used in the repair of stalled replication forks.

In summary, we have further developed the established p^{un} mouse model for measuring HR by making it applicable to conditional mouse models. This has allowed us to investigate the role of *Blm* and *Brca1*, two essential mouse genes, in HR. Furthermore, we have provided insight into the various types of HR mechanisms responsible for deletion-mediated reversion events that can be detected by using this *in vivo* mouse model.

ACKNOWLEDGMENTS

This work was supported by the National Institute of Environmental Health Sciences (grant K22ES012264 to A.J.R.B.), an American Cancer Society Institutional Research Grant (ACS-IRG-00-173-04) pilot project award (to A.J.R.B.), and the National Institute of Aging (grant T32AG021890 to A.D.B.).

We thank Jo Ann Martinez for helping to establish the mouse lines.

REFERENCES

1. **Adams, M. D., M. McVey, and J. J. Sekelsky.** 2003. Drosophila BLM in double-strand break repair by synthesis-dependent strand annealing. Science **299:**265–267.
2. **Ames, B. N., M. K. Shigenaga, and T. M. Hagen.** 1993. Oxidants, antioxidants, and the degenerative diseases of aging. Proc. Natl. Acad. Sci. U. S. A. **90:**7915–7922.
3. **Babbe, H., N. Chester, P. Leder, and B. Reizis.** 2007. The Bloom's syndrome helicase is critical for development and function of the alphabeta T-cell lineage. Mol. Cell. Biol. **27:**1947–1959.
4. **Bast, R. C., Jr., and G. B. Mills.** 2010. Personalizing therapy for ovarian cancer: BRCAness and beyond. J. Clin. Oncol. **28:**3545–3548.
5. **Bischof, O., et al.** 2001. Regulation and localization of the Bloom syndrome protein in response to DNA damage. J. Cell Biol. **153:**367–380.
6. **Bishop, A. J., et al.** 2003. Atm-, p53-, and Gadd45a-deficient mice show an increased frequency of homologous recombination at different stages during development. Cancer Res. **63:**5335–5343.
7. **Bishop, A. J., B. Kosaras, N. Carls, R. L. Sidman, and R. H. Schiestl.** 2001. Susceptibility of proliferating cells to benzo[a]pyrene-induced homologous recombination in mice. Carcinogenesis **22:**641–649.
8. **Bishop, A. J., B. Kosaras, R. L. Sidman, and R. H. Schiestl.** 2000. Benzo-(a)pyrene and X-rays induce reversions of the pink-eyed unstable mutation in the retinal pigment epithelium of mice. Mutat. Res. **457:**31–40.
9. **Bishop, A. J., and R. H. Schiestl.** 2001. Homologous recombination as a mechanism of carcinogenesis. Biochim. Biophys. Acta **1471:**M109–M121.
10. **Bodenstein, L., and R. L. Sidman.** 1987. Growth and development of the mouse retinal pigment epithelium. II. Cell patterning in experimental chimaeras and mosaics. Dev. Biol. **121:**205–219.
11. **Bouwman, P., and J. Jonkers.** 2008. Mouse models for BRCA1 associated tumorigenesis: from fundamental insights to preclinical utility. Cell Cycle **7:**2647–2653.
12. **Branda, C. S., and S. M. Dymecki.** 2004. Talking about a revolution: the impact of site-specific recombinases on genetic analyses in mice. Dev. Cell **6:**7–28.
13. **Brilliant, M. H.** 2001. The mouse p (pink-eyed dilution) and human P genes, oculocutaneous albinism type 2 (OCA2), and melanosomal pH. Pigment Cell Res. **14:**86–93.
14. **Brilliant, M. H., Y. Gondo, and E. M. Eicher.** 1991. Direct molecular identification of the mouse pink-eyed unstable mutation by genome scanning. Science **252:**566–569.
15. **Broberg, K., et al.** 2009. Association between polymorphisms in RMI1, TOP3A, and BLM and risk of cancer, a case-control study. BMC Cancer **9:**140.
16. **Brose, M. S., et al.** 2002. Cancer risk estimates for BRCA1 mutation carriers identified in a risk evaluation program. J. Natl. Cancer Inst. **94:**1365–1372.
17. **Brown, A. D., A. B. Claybon, and A. J. R. Bishop.** 2010. Mouse WRN helicase domain is not required for spontaneous homologous recombination-mediated DNA deletion. J. Nucleic Acids. **2010:**356917.
18. **Brown, A. D., B. Karia, A. M. Wiles, and A. J. R. Bishop.** 2008. The intertwining of DNA damage response pathway components and homologous recombination repair, p. 1–68. *In* J. H. Schultz (ed.), Genetic recombination research progress. Nova Science Publishers, Inc., New York, NY.
19. **Chaganti, R. S., S. Schonberg, and J. German.** 1974. A manyfold increase in sister chromatid exchanges in Bloom's syndrome lymphocytes. Proc. Natl. Acad. Sci. U. S. A. **71:**4508–4512.
20. **Chen, J., et al.** 1998. Stable interaction between the products of the BRCA1 and BRCA2 tumor suppressor genes in mitotic and meiotic cells. Mol. Cell **2:**317–328.
21. **Chen, Y., et al.** 1996. BRCA1 is a 220-kDa nuclear phosphoprotein that is expressed and phosphorylated in a cell cycle-dependent manner. Cancer Res. **56:**3168–3172.
22. **Cheok, C. F., L. Wu, P. L. Garcia, P. Janscak, and I. D. Hickson.** 2005. The Bloom's syndrome helicase promotes the annealing of complementary single-stranded DNA. Nucleic Acids Res. **33:**3932–3941.
23. **Chester, N., H. Babbe, J. Pinkas, C. Manning, and P. Leder.** 2006. Mutation of the murine Bloom's syndrome gene produces global genome destabilization. Mol. Cell. Biol. **26:**6713–6726.
24. **Chester, N., F. Kuo, C. Kozak, C. D. O'Hara, and P. Leder.** 1998. Stage-specific apoptosis, developmental delay, and embryonic lethality in mice homozygous for a targeted disruption in the murine Bloom's syndrome gene. Genes Dev. **12:**3382–3393.
25. **Chu, W. K., and I. D. Hickson.** 2009. RecQ helicases: multifunctional genome caretakers. Nat. Rev. Cancer **9:**644–654.
26. **Claybon, A. B., B. B. C. Karia, and A. J. R. Bishop.** 2010. PARP1 suppresses homologous recombination events in mice in vivo. Nucleic Acids Res. **38:**7538–7545.
27. **Cortez, D., Y. Wang, J. Qin, and S. J. Elledge.** 1999. Requirement of ATM-dependent phosphorylation of brca1 in the DNA damage response to double-strand breaks. Science **286:**1162–1166.
28. **Devilee, P., et al.** 1993. Linkage to markers for the chromosome region 17q12-q21 in 13 Dutch breast cancer kindreds. Am. J. Hum. Genet. **52:**730–735.
29. **Drew, Y., and R. Plummer.** 2010. The emerging potential of poly(ADP-ribose) polymerase inhibitors in the treatment of breast cancer. Curr. Opin. Obstet. Gynecol. **22:**67–71.
30. **Easton, D. F., D. Ford, and D. T. Bishop.** 1995. Breast and ovarian cancer incidence in BRCA1-mutation carriers. Breast Cancer Linkage Consortium. Am. J. Hum. Genet. **56:**265–271.
31. **Ellis, N. A., and J. German.** 1996. Molecular genetics of Bloom's syndrome. Hum. Mol. Genet. **5 Spec No:**1457–1463.
32. **Ellis, N. A., et al.** 1995. The Bloom's syndrome gene product is homologous to RecQ helicases. Cell **83:**655–666.
33. **Ershov, A. V., and O. G. Stroeva.** 1989. Post-natal pattern of cell proliferation in retinal pigment epithelium of mice studied with tritiated thymidine autoradiography. Cell Differ. Dev. **28:**173–177.
34. **Farago, A. F., R. B. Awatramani, and S. M. Dymecki.** 2006. Assembly of the

brainstem cochlear nuclear complex is revealed by intersectional and subtractive genetic fate maps. Neuron **50:**205–218.
35. **Ford, D., D. F. Easton, D. T. Bishop, S. A. Narod, and D. E. Goldgar.** 1994. Risks of cancer in BRCA1-mutation carriers. Breast Cancer Linkage Consortium. Lancet **343:**692–695.
36. **Foster, F. S., M. Zhang, A. S. Duckett, V. Cucevic, and C. J. Pavlin.** 2003. In vivo imaging of embryonic development in the mouse eye by ultrasound biomicroscopy. Invest. Ophthalmol. Vis. Sci. **44:**2361–2366.
37. **Galli, A., and R. H. Schiestl.** 1995. On the mechanism of UV and gamma-ray-induced intrachromosomal recombination in yeast cells synchronized in different stages of the cell cycle. Mol. Gen. Genet. **248:**301–310.
38. **German, J.** 1997. Bloom's syndrome. XX. The first 100 cancers. Cancer Genet. Cytogenet. **93:**100–106.
39. **German, J., and E. Passarge.** 1989. Bloom's syndrome. XII. Report from the registry for 1987. Clin. Genet. **35:**57–69.
40. **Gondo, Y., et al.** 1993. High-frequency genetic reversion mediated by a DNA duplication: the mouse pink-eyed unstable mutation. Proc. Natl. Acad. Sci. U. S. A. **90:**297–301.
41. **Gudas, J. M., et al.** 1996. Cell cycle regulation of BRCA1 mRNA in human breast epithelial cells. Cell Growth Differ. **7:**717–723.
42. **Haber, J. E.** 1999. DNA recombination: the replication connection. Trends Biochem. Sci. **24:**271–275.
43. **Haber, J. E., G. Ira, A. Malkova, and N. Sugawara.** 2004. Repairing a double-strand chromosome break by homologous recombination: revisiting Robin Holliday's model. Philos. Trans. R. Soc. Lond. B Biol. Sci. **359:**79–86.
44. **Hanada, K., and I. D. Hickson.** 2007. Molecular genetics of RecQ helicase disorders. Cell. Mol. Life Sci. **64:**2306–2322.
45. **Helleday, T., J. Lo, D. C. van Gent, and B. P. Engelward.** 2007. DNA double-strand break repair: from mechanistic understanding to cancer treatment. DNA Repair (Amst.) **6:**923–935.
46. **Hendricks, C. A., et al.** 2003. Spontaneous mitotic homologous recombination at an enhanced yellow fluorescent protein (EYFP) cDNA direct repeat in transgenic mice. Proc. Natl. Acad. Sci. U. S. A. **100:**6325–6330.
47. **Jin, Y., et al.** 1997. Cell cycle-dependent colocalization of BARD1 and BRCA1 proteins in discrete nuclear domains. Proc. Natl. Acad. Sci. U. S. A. **94:**12075–12080.
48. **Karow, J. K., A. Constantinou, J. L. Li, S. C. West, and I. D. Hickson.** 2000. The Bloom's syndrome gene product promotes branch migration of holliday junctions. Proc. Natl. Acad. Sci. U. S. A. **97:**6504–6508.
49. **MacGregor, G. R., B. P. Zambrowicz, and P. Soriano.** 1995. Tissue non-specific alkaline phosphatase is expressed in both embryonic and extraembryonic lineages during mouse embryogenesis but is not required for migration of primordial germ cells. Development **121:**1487–1496.
50. **Machwe, A., L. Xiao, J. Groden, S. W. Matson, and D. K. Orren.** 2005. RecQ family members combine strand pairing and unwinding activities to catalyze strand exchange. J. Biol. Chem. **280:**23397–23407.
51. **Machwe, A., L. Xiao, J. Groden, and D. K. Orren.** 2006. The Werner and Bloom syndrome proteins catalyze regression of a model replication fork. Biochemistry **45:**13939–13946.
52. **McVey, M., J. R. Larocque, M. D. Adams, and J. J. Sekelsky.** 2004. Formation of deletions during double-strand break repair in Drosophila DmBlm mutants occurs after strand invasion. Proc. Natl. Acad. Sci. U. S. A. **101:** 15694–15699.
53. **Miki, Y., et al.** 1994. A strong candidate for the breast and ovarian cancer susceptibility gene BRCA1. Science **266:**66–71.
54. **Mohaghegh, P., J. K. Karow, R. M. Brosh, Jr., V. A. Bohr, and I. D. Hickson.** 2001. The Bloom's and Werner's syndrome proteins are DNA structure-specific helicases. Nucleic Acids Res. **29:**2843–2849.
55. **Mori, M., D. Metzger, J. M. Garnier, P. Chambon, and M. Mark.** 2002. Site-specific somatic mutagenesis in the retinal pigment epithelium. Invest. Ophthalmol. Vis. Sci. **43:**1384–1388.
56. **Moynahan, M. E., J. W. Chiu, B. H. Koller, and M. Jasin.** 1999. Brca1 controls homology-directed DNA repair. Mol. Cell **4:**511–518.
57. **Moynahan, M. E., T. Y. Cui, and M. Jasin.** 2001. Homology-directed DNA repair, mitomycin-c resistance, and chromosome stability is restored with correction of a Brca1 mutation. Cancer Res. **61:**4842–4850.
58. **Moynahan, M. E., and M. Jasin.** 2010. Mitotic homologous recombination maintains genomic stability and suppresses tumorigenesis. Nat. Rev. Mol. Cell. Biol. **11:**196–207.
59. **Nakayama, A., et al.** 1998. Mutations in microphthalmia, the mouse homolog of the human deafness gene MITF, affect neuroepithelial and neural crest-derived melanocytes differently. Mech. Dev. **70:**155–166.
60. **Oetting, W. S., and R. A. King.** 1999. Molecular basis of albinism: mutations and polymorphisms of pigmentation genes associated with albinism. Hum. Mutat. **13:**99–115.
61. **Ralf, C., I. D. Hickson, and L. Wu.** 2006. The Bloom's syndrome helicase can promote the regression of a model replication fork. J. Biol. Chem. **281:** 22839–22846.
62. **Raymond, S. M., and I. J. Jackson.** 1995. The retinal pigmented epithelium is required for development and maintenance of the mouse neural retina. Curr. Biol. **5:**1286–1295.
63. **Russell, P. J., and B. Pierce.** 2000. Fundamentals of genetics. Benjamin-Cummings Publishing Company, San Francisco, CA.
64. **Scully, R., et al.** 1997. Association of BRCA1 with Rad51 in mitotic and meiotic cells. Cell **88:**265–275.
65. **Shen, S. X., et al.** 1998. A targeted disruption of the murine Brca1 gene causes gamma-irradiation hypersensitivity and genetic instability. Oncogene **17:**3115–3124.
66. **Sonoda, E., et al.** 1999. Sister chromatid exchanges are mediated by homologous recombination in vertebrate cells. Mol. Cell. Biol. **19:**5166–5169.
67. **Stark, J. M., A. J. Pierce, J. Oh, A. Pastink, and M. Jasin.** 2004. Genetic steps of mammalian homologous repair with distinct mutagenic consequences. Mol. Cell. Biol. **24:**9305–9316.
68. **Thakur, S., et al.** 1997. Localization of BRCA1 and a splice variant identifies the nuclear localization signal. Mol. Cell. Biol. **17:**444–452.
69. **Thyagarajan, B., M. J. Guimaraes, A. C. Groth, and M. P. Calos.** 2000. Mammalian genomes contain active recombinase recognition sites. Gene **244:**47–54.
70. **Vaughn, J. P., et al.** 1996. BRCA1 expression is induced before DNA synthesis in both normal and tumor-derived breast cells. Cell Growth Differ. **7:**711–715.
71. **Wang, X.** 2009. Cre transgenic mouse lines. Methods Mol. Biol. **561:**265–273.
72. **Wang, Y., et al.** 2000. BASC, a super complex of BRCA1-associated proteins involved in the recognition and repair of aberrant DNA structures. Genes Dev. **14:**927–939.
73. **Wang, Y., K. Smith, B. C. Waldman, and A. S. Waldman.** Depletion of the bloom syndrome helicase stimulates homology-dependent repair at double-strand breaks in human chromosomes. DNA Repair (Amst.) **10:**416–426.
74. **Wilson, C. A., et al.** 1997. Differential subcellular localization, expression and biological toxicity of BRCA1 and the splice variant BRCA1-delta11b. Oncogene **14:**1–16.
75. **Wooster, R., and B. L. Weber.** 2003. Breast and ovarian cancer. N. Engl. J. Med. **348:**2339–2347.
76. **Wu, L., S. L. Davies, N. C. Levitt, and I. D. Hickson.** 2001. Potential role for the BLM helicase in recombinational repair via a conserved interaction with RAD51. J. Biol. Chem. **276:**19375–19381.
77. **Xu, X., et al.** 2001. Genetic interactions between tumor suppressors Brca1 and p53 in apoptosis, cell cycle and tumorigenesis. Nat. Genet. **28:**266–271.
78. **Xu, X., et al.** 1999. Conditional mutation of Brca1 in mammary epithelial cells results in blunted ductal morphogenesis and tumour formation. Nat. Genet. **22:**37–43.
79. **Zhang, F., et al.** 2009. PALB2 links BRCA1 and BRCA2 in the DNA-damage response. Curr. Biol. **19:**524–529.
80. **Zhang, J., et al.** 2004. Chk2 phosphorylation of BRCA1 regulates DNA double-strand break repair. Mol. Cell. Biol. **24:**708–718.
81. **Zhong, Q., et al.** 1999. Association of BRCA1 with the hRad50-hMre11-p95 complex and the DNA damage response. Science **285:**747–750.